Role of 3d electrons in the rapid suppression of superconductivity in the dilute V doped spinel superconductor $LiTi_2O_4$

2011 Supercond. Sci. Technol. 24 115007

(http://iopscience.iop.org/0953-2048/24/11/115007)

Supercond. Sci. Technol. **24** (2011) 115007 (7pp) doi:10.1088/0953-2048/24/11/115007

Role of 3d electrons in the rapid suppression of superconductivity in the dilute V doped spinel superconductor $LiTi_2O_4$

C L Chen[1], C L Dong[2], K Asokan[3], J L Chen[4], Y S Liu[4], J-H Guo[5], W L Yang[5], Y Y Chen[1], F C Hsu[1], C L Chang[4] and M K Wu[1]

[1] Institute of Physics, Academia Sinica, Taipei 11529, Taiwan
[2] National Synchrotron Radiation Research Center, Hsinchu 30076, Taiwan
[3] Inter-University Accelerator Centre, Aruna Asaf Ali Marg, New Delhi-110067, India
[4] Department of Physics, Tamkang University, Tamsui, Taipei County, Taiwan
[5] Advanced Light Source, Lawrence Berkeley National Laboratory, Berkeley, CA 94720, USA

E-mail: clchen@phys.sinica.edu.tw and dong.cl@nsrrc.org.tw

Received 28 June 2011, in final form 5 September 2011
Published 30 September 2011
Online at stacks.iop.org/SUST/24/115007

Abstract
The microscopic effects of V doping in $LiTi_2O_4$ have been poorly understood. The present study employs x-ray absorption near-edge structure (XANES) and resonant inelastic soft-x-ray scattering (RIXS) spectroscopy to understand the change in the electronic structure due to dilute V doping in spinel $LiTi_2O_4$ and the possible origin for the rapid suppression of superconductivity in these compounds. Results from the XANES spectra at Ti L and K edges and Ti L-RIXS show that Ti exists in a mixed-valence state and, with V doping, the unoccupied states of Ti in the t_{2g} band increase. The rapid suppression of superconductivity is associated with the change in Ti 3d electrons and Ti–O hybridization.

(Some figures in this article are in colour only in the electronic version)

1. Introduction

Extensive research concerning high T_c superconductivity has been focused mainly in the family of cuprates, and their origin has been considered to be one with unconventional nature. Experimental results, especially from high energy electron spectroscopies, show that the mixed-valence nature of Cu ions is responsible for high T_c superconductivity. Similar to cuprates [1, 2], titanates exhibit mixed-valence nature in their ground state. One of the Ti based superconductors is $LiTi_2O_4$ (LTO), considered as an exotic superconductor, with transition temperature (T_c) $\sim$ 12 K [3, 4]. However, the mechanism of superconductivity is as yet an open issue. $LiTi_2O_4$ has been reported to be a BCS superconductor, resonating valence bond (RVB) or bipolaronic and more recently an exotic superconductor. LTO as a mixed-valence compound contains an equal ratio of Ti^{3+}, which has spin $S = 1/2$, and Ti^{4+}, which has $S = 0$. This is the only known oxide spinel superconductor to date. In general, spinel oxides with 3d transition metals on the octahedral sites are known to exhibit ferromagnetism, antiferromagnetism, charge ordering, and other types of magnetic and electronic ordering depending on the average valence of the cations. LiV_2O_4 (LVO) is an isostructural compound which is the closest neighbour to LTO and is also a mixed-valence system with equal ratio of V^{3+} ($S = 1$) and V^{4+} ($S = 1/2$). It is not a superconductor but exhibits heavy fermionic behaviour. It is well known that magnetic impurities do suppress the superconductivity in many materials. Therefore, it will be of interest to investigate whether dilute doping of magnetic ions in LTO would result in complete suppression of superconductivity. Such a study may provide a clue for the mechanism of superconductivity. A rapid suppression of superconducting transition temperature (T_c) was observed in the magnetic ion doped system $LiTi_{1-x}M_xO_4$ (M = Cr, V and Mn). Vanadium (V) was found to be more effective in T_c reduction even at small concentrations [5]. It is

known that the magnetic moment of V is much smaller than that of Mn and Cr. These results imply that, apart from the role of magnetic moments, there are other mechanisms to account for this giant T_c suppression. It has been observed that even 2% of V doping in LTO results in the reduction of T_c from ∼13 to ∼5 K [5–8]. Such suppression of superconducting behaviour in LTO might unravel the mechanism of superconductivity. The investigation of the atomic and electronic structure of materials in general has clarified our understanding of their transport properties. In this regard, previous studies have been performed on the electronic structure of LTO [9, 10]. The suppression of superconductivity in V doped LTO is discussed on the basis of a pair-breaking mechanism [6]; crystalline distortion from octahedral symmetry [11] and the variation of Ti and V valence states were suggested to be closely related to its physical properties. The interaction between electrons cannot be ignored as V ions become doped into the structures [12]. X-ray absorption near-edge structure (XANES) spectroscopy is a sensitive tool that probes unoccupied electronic states above the Fermi level (E_F) and the structural symmetry of mixed-oxide systems [13, 14] with respect to the crystallographic structure and the electronic-orbital interaction from the hybridization states of the 3d transition metal. Thus XANES at the Ti L and K edges determines the electronic structure of mixed-valence states of Ti in the V doped LTO. Doping of V ions in the octahedral site is expected to distort the crystal and thus to affect the bonding of O–Ti(V)–O and the unoccupied density of states of 3d orbitals [11]. Resonant inelastic x-ray scattering (RIXS) is yet another x-ray spectroscopic technique used to investigate the electronic structure of materials and correlate with XANES results. RIXS spectra probe the de-excitation of the x-ray absorption final state and provide information about the ground state of the system through the intermediate excited states. By proper tuning of the excitation energy, specific RIXS features are significantly enhanced, corresponding to electronic configurations in the mixed ground states [15–17]. RIXS is therefore a complementary tool to XANES. Besides, the final state of RIXS has the same symmetry as the initial state of the x-ray absorption process; a forbidden electronic transition such as d–d excitations can be measured as two dipole transitions are involved. The RIXS spectra at TM L edges reflect the 3d partial density of states. In particular, it probes the energy correlation in strongly correlated materials [18–20] in terms of a local excitation (e.g. d–d excitation), in which the transition occurs between the 3d valence and the conduction bands, as well as the charge transfer for the transition from an occupied O 2p state to an unoccupied metal 3d states. RIXS is commonly used for studies of transition metal oxide (TMO) compounds because its resonance spectra provide well defined features with larger intensities. Since XANES and RIXS are element and orbital specific, combination of these techniques at the Ti $L_{2,3}$ absorption edges would provide significant information about the electronic structures of these spinel superconductors. This approach is ideal in all 3d transition metal compounds, because the resonant excitation and de-excitation allow us to measure the energy of excited states, so called d–d excitations, which otherwise is unreachable by direct electric dipole transitions and where the variations in x-ray absorption processes are not significant with changes in composition.

The present study uses both XANES and RIXS spectroscopies to understand the effect of V doping on the electronic properties of the LTO system and the cause of the rapid suppression of superconductivity.

2. Experimental details

All samples reported in this study, $Li(Ti_{1-x}V_x)_2O_4$ ($x = 0, 0.05, 0.01, 0.015$ and 0.02), were synthesized by a conventional two-step solid-state reaction route using high purity oxides of TiO_2, $LiCO_3$, and V_2O_3 reported in detail elsewhere [6–8]. The powder x-ray diffraction (XRD) patterns [7] were used to confirm the phase purity and to understand the variation of lattice parameters as a function of V doping. Since the interest was to understand the effect of dilute doping, concentrations up to 2% were selected. It is expected that oxygen stoichiometry remains the same for all these dilute concentrations as the preparation was the same. The XANES at the Ti L and K edges were measured in the beamlines HSGM (20A1) and wiggler-C (17C), respectively, at the National Synchrotron Radiation Research Center (NSRRC), Taiwan. The XANES spectra at the Ti L edge were measured in the total-electron-yield (TEY) mode at 295 K with the pressure $\sim 5 \times 10^{-9}$ Torr in the ultrahigh vacuum chamber. The Ti K-edge spectra were recorded with an interval of 0.3 eV for the XANES in the fluorescence yield mode at room temperature. All spectra were normalized by the following standard procedure. The metal foils and oxide powders, TiO_2 and Ti_2O_3, were used for energy calibration and also for comparison of spectra of various electronic valence states. The x-ray emission experiments were performed at beamline 7.0.1 at the Advanced Light Source (ALS), Lawrence Berkeley National Laboratory (LBNL). The beamline is equipped with a 99-pole, 5 cm period undulator and a spherical grating monochromator [21]. The RIXS spectra were recorded with a high-resolution grating spectrometer at grazing incidence with a two-dimensional detector [22]; the resolution was set at 0.4 eV for Ti L emission spectra. The resolution of the monochromator was set the same as for the emission measurements.

3. Results and discussion

X-ray diffraction patterns of $Li(Ti_{1-x}V_x)_2O_4$ ($x = 0, 0.05, 0.01, 0.015$ and 0.02) are shown in figure 1. These patterns reflect that the crystal structure is of pure spinel structure without any impurity phases and the lattice constant decreases with x. The chemical analysis determined by ICP-AES was found to be consistent with the nominal composition [6–8]. Doping smaller ionic radius of V at the Ti site resulted in the change of the lattice constant. The inset of figure 1 shows the crystal structure of LTO, which belongs to cubic space group $Fd3m$, with lattice parameter $a = 8.404$ Å and eight AB_2O_4 units per unit cell. The Li ions are located at 8a tetrahedral (T_d) A sites, Ti ions at 16d octahedral (O_h) B sites,

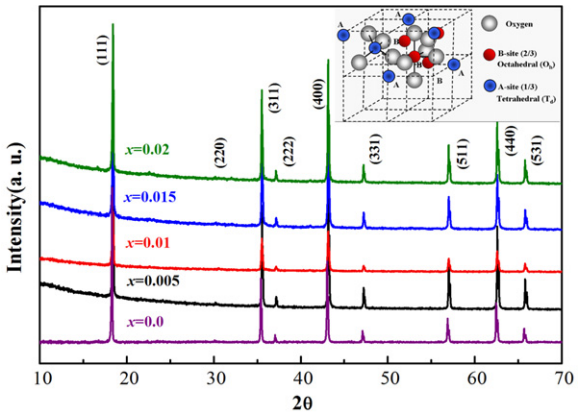

Figure 1. The x-ray diffraction pattern of $LiTi_{2-x}V_xO_4$. All diffraction peaks are indexed with a pure spinel structure. The inset shows the crystal structure of LTO, with spheres Li black, Ti red, and O white for the respective ion.

and oxide ions at 32e sites. The electronic structure is believed to depend strongly on the hybridization of the transition metal (TM) 3d–O 2p orbitals about the E_F, at which electronic exchange typically occurs. The altered electronic structure around TM ions thus has greater influence on their oxidation state and physical properties. Understanding the physical properties of AB_2O_4 with mixed-valence states requires a complete knowledge of their electronic structure, particularly the spin–orbital symmetry and the p–d hybridization in the unoccupied states. Several experiments and theories indicate that AB_2O_4 exhibits strong electron–hole correlations due to TM ions at various sites [9, 10]. To investigate the effects of dilute doping of V in LTO, the XANES and RIXS at Ti L edges were measured. As evident from the inset of figure 2, the Ti L-edge XANES spectra show several well resolved features that are due to excitations of a 2p core electron into the Ti 3d empty states, i.e., a transition from the ground state with configuration $2p^63d^n$ to an excited electronic configuration $2p^53d^{n+1}$ with various multiplet excitations. As a result of spin–orbital coupling in the transition metal 2p state, the spectra display two prominent features in the energy ranges 455–461 eV and 461.2–468 eV, corresponding to the L_3 ($2p_{3/2} \rightarrow 3d$) and L_2 ($2p_{1/2} \rightarrow 3d$) absorptions respectively. The multiple structures are due to the strong coulomb interaction between poorly screened Ti 3d electrons and the Ti 2p core hole [14]. The L_2 edge features are broadened relative to the L_3 edge because of a shorter lifetime of the $2p_{1/2}$ core hole (i.e. a radiationless electron transition from $2p_{3/2}$ to the $2p_{1/2}$ level), accompanied by the promotion of a valence electron into the conduction band. Under the O_h crystal field, the 3d band splits into t_{2g} (formed by d_{xy}, d_{xz}, and d_{yz} orbitals) and e_g (formed by $d_{x^2-y^2}$ and $3d_{3z^2-r^2}$) subbands ($\Delta = (e_g) - (t_{2g}) = 10$ Dq). Due to crystal-field splitting, the L_3-edge feature possesses t_{2g} and e_g bands. Ti 3d RIXS spectra of LTO and 2% V doped LTO are displayed with energy loss scales in figure 2(a). The energy loss spectrum is obtained by subtracting the energy of the emitted photons from the incoming photon energy (excitation energy). This energy is selected based on XANES Ti L-edge spectra. Compounds of TMO exhibit four common features in RIXS spectra: (i) sharp d–d excitations within the gap (<4 eV), (ii) broad maxima around 5 eV, (iii) continuous features in 8–12 eV, and (iv) a feature showing a large dispersion at energy > 12 eV. The spectral variations for various excitation energies (letters a–k) and doping levels are evident in figure 2. Different photon energies were used to collect the emission spectra which are marked by arrows (letters a–k) in the XANES spectra as shown in the inset of figure 2. For example, spectrum b was obtained by using the incident photon energy of 457 eV (L_3 peak maximum). The first feature corresponds to an elastic scattering feature that occurs at 0 eV corresponding to incoming photon energy. The inelastic scattering features in the range of 5–10 eV originate in the complex charge transfer excitation from O 2p to Ti 3d t_{2g} and

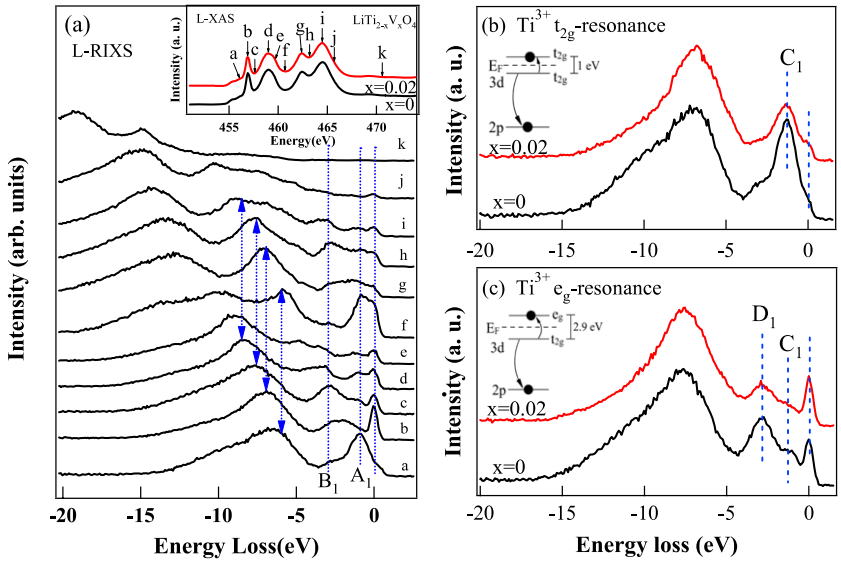

Figure 2. (a) Ti L-RIXS spectra of $LiTi_2O_4$ recorded with various excitation energies, marked by the letters (a–k) in the Ti L-XANES spectrum shown in the inset. Ti L_3 RIXS spectra of $LiTi_{2-x}V_xO_4$ ($x = 0$ and 0.02), at (b) Ti^{3+} t_{2g}-resonance, and (c) Ti^{3+} e_g-resonance. The insets of (b) and (c) show the energy diagram of the d–d excitation.

e_g subbands [20, 23]. Several low energy inelastic scattering features are also observed at energy < 5 eV, which are absent from TiO_2 [19]. Note that the spectra in this energy range significantly differ from that of TiO_2. The energy loss features presented above arise due to the presence of Ti^{3+} giving rise to an electron in the 3d state, implying that 3d t_{2g} orbitals are occupied. The intensity of the d–d excitations (A_1 and B_1) changes significantly at the particular excitation energies, implying the strong electron correlation of the d electrons. In the RIXS spectrum (a), a strong energy loss feature is seen at ∼1 eV. Tuning the excitation energy at resonance energy corresponding to the peak position (b) in XANES, the intensity of the energy loss feature reduces. Further increase in the excitation energy (in the valley region marked as c) shows an enhancement of the energy loss feature at ∼2.9 eV. Generally, the criterion for the selection of excitation energy for RIXS is based on the resonance energy obtained from the XANES feature. It is quite uncommon that when the excitation energy is tuned below the L_3 t_{2g} peak in spectrum (a) it results in enhancement of the inelastic scattering A_1. In addition, this enhancement of the inelastic part is not observed at either the t_{2g} (b) or e_g (d) resonance energy. This is understood if one considers the presence of Ti^{3+} contributions as revealed by the constant initial state (CIS) absorption spectrum [21]. XANES spectral profiles are quite similar for both LTO and V doped LTO, and the spectral changes are marginally small. When the spectral changes of XANES are small with doping, the analyses rely on the spectral deconvolution and the specific electronic state measured separately from RIXS [17]. As a result, at the particular energy (c), an enhancement of the Ti^{3+} contribution is observed where there is a dip in the Ti^{4+} spectrum (between t_{2g} and e_g). Therefore, two excitation energies, 456 and 457.5 eV, which correspond, respectively, to the Ti^{3+} t_{2g}- and e_g-resonance energies, were displayed in figures 2(b) and (c) [21].

The low energy excited feature C_1 at ∼1 eV (see figures 2(b) and (c)) is resonantly enhanced when the excitation energy is tuned to the t_{2g} resonance. This feature corresponds to the electron–hole pairs within the t_{2g} band. When the excitation energy was set to the e_g resonance (figure 2(c)), D_1 was enhanced, which corresponds to the transition from the occupied t_{2g} band to the unoccupied e_g band. The presence of such an RIXS feature suggests strong electron–electron correlation. This energy loss feature at ∼2.9 eV of the d–d transition represents the magnitude of the crystal-field splitting, 10 Dq, and it refers to the ground state without the core hole. Comparison of the spectra of each set shows that, as the doping concentration increases ($x = 0.02$), the intensity of the loss features decreases. Hence fewer electrons are distributed in the t_{2g} band. In addition, in previous work on TiO_2 no intensity was observed in this region below the elastic peak [20]. The variation of the intensity is therefore due to the change of the partially filled t_{2g} band that arising from the doping effect of the V. This result strongly suggests that the Ti valence is enhanced with V doping. The active transition metal ion, Ti, in $LiTi_2O_4$ has a formal valence state of 3+ and 4+ with ∼0.5 electrons in the d orbital and hence has a lower electronic density. Doping V results in reduction in the number of Ti 3d electrons. This implies an increase in the formal valence of the Ti ion. In other words, in LTO, Ti is in a mixed-valence state and contains some t_{2g} electrons. If there is no t_{2g} electron, d–d excitation will be absent since there is no electron in t_{2g} that can be excited to the unoccupied t_{2g} or e_g states. Any variation in valence of Ti is thus reflected in the RIXS spectra. Absence or reduction of features in the energy range 0–5 eV implies reduction of d–d transitions. As the Ti valence changes from +4 to +3, there are more electrons occupying the t_{2g} orbital. Thus, the possibility of the excitation of the t_{2g} electron into the unoccupied t_{2g} or e_g states is increased. The d–d excitation (t_{2g}–t_{2g} and t_{2g}–e_g) in the spectra is only observed in RIXS and not in XANES. The greatest importance of seeing this d–d excitation is that the t_{2g} occupation number is changed after V doping. In other words, with V doping, t_{2g} electrons are reduced and this valence variation is significantly observed in the spectrum of RIXS.

To obtain the complementary information, detailed analysis of Ti L-edge XANES was investigated. The Ti $L_{3,2}$-edge XANES spectra of $LiTi_{1-x}V_xO_4$ (or LTVO) ($x = 0$–0.02), along with reference oxides TiO_2 (anatase) and Ti_2O_3, are presented in figure 3(a). The shapes of the spectra of LTO undoped and after dilute V doping ($x = 0.005$) are very similar. Peaks A_2 and B_2 (C_2 and E_2) were previously assigned as the t_{2g} (e_g) states of the crystal-field split 3d orbitals. The 10 Dq crystal-field splitting is near 1.8 eV, but the splitting increases from 1.8 to 2.0 eV as the doping with V increases from $x = 0.005$ to 0.02. This effect reflects the distortion of O_h symmetry when the Ti is substituted by a smaller V ion. This is consistent with the powder XRD results and theoretical calculations of electronic structure [14, 24, 25]. Furthermore, the B_2 peak broadens as the V is gradually doped. As earlier reported [14, 24, 25], due to the Jahn–Teller distortion with ΔE_{J-T} energy splitting in the e_g band, the Ti e_g orbitals point directly towards the 2p orbitals of the octahedrally coordinated O atoms. The e_g band is sensitive to the local environment, leading to an altered bonding angle/distance of O–Ti–O in the presence of V doping. The e_g-related peaks are also broader than the t_{2g} peak because of greater hybridization between Ti e_g orbitals and O ligand states and associated effects of solid-state broadening [14]. The e_g peak shows a narrow and symmetric profile in the undoped LTO, indicating symmetrical octahedrally coordinated Ti–O bonds. It becomes broad and asymmetric with the doping, implying distortion by the presence of V doping. This distortion may arise from the uneven Ti–O bonds in the octahedral environment. The e_g peak on the higher energy side originates from the short Ti–O bonds due to a hybridization effect becoming stronger (compared to the long Ti–O bonds), so that the intensity ratio of the higher energy to lower energy e_g peaks is increased with the V doping, implying the long Ti–O bonds are decreased [22]. In addition, an increase in the integrated area under the peak A_2 represents the increase of the Ti 3d unoccupied states, implying the valence of Ti to be increased upon V doping. The electronic configuration of Ti from the Ti–O bond exhibits a combination of $3d^0$ ($t_{2g}^0 e_g^0$) and $3d^1$ ($t_{2g}^1 e^0$) in the ground state. Figure 3(b) shows the integrated area of the ratio A_2/B_2; this ratio clearly increases as the doping with V increases. The more intense

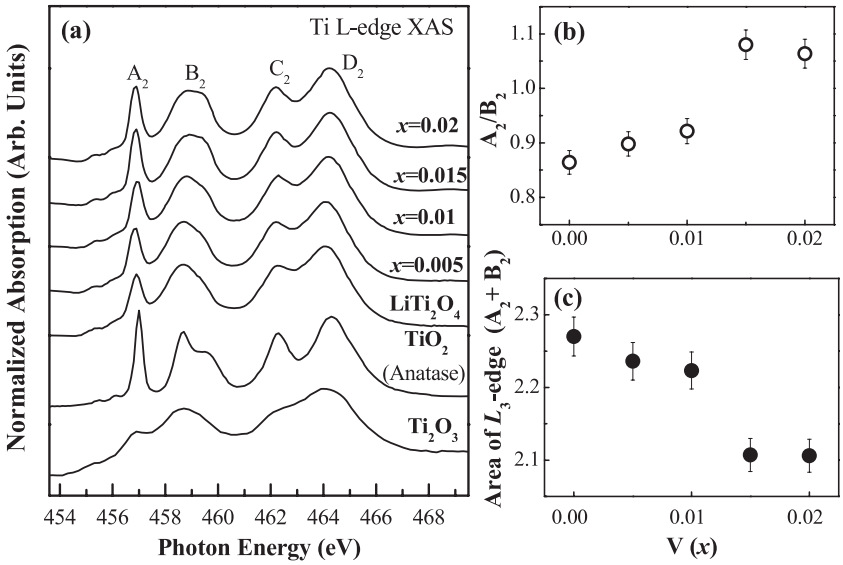

Figure 3. (a) Ti $L_{3,2}$-edge (2p → 3d) XANES spectra for $LiTi_{2-x}V_xO_4$ ($x = 0.005$–0.02), $LiTi_2O_4$ ($x = 0$), TiO_2 and Ti_2O_3. (b) The ratio of integrated area A_2/B_2 under the pre-peaks. The increase of the ratio implies the presence of $3d^0$ states. (c) The area $A_2 + B_2$ decreases as the V concentration increases due to the V replacing the Ti.

A_2 (t_{2g}) feature implies an increased oxidation state and thus indicates the presence of Ti^{4+} ($3d^0$) [26, 27]. Moreover, the area of the L_3- edge, which corresponds to ($A_2 + B_2$), decreases progressively as the V concentration increases, as shown in figure 3(c). This is due to the fact that V replaces the Ti, which is in accordance with the XRD results [7]. The increasing of Ti valence upon V doping is observed in the Ti 2p XANES, although it is very small but real, and this is strongly evident in the Ti 2p RIXS spectra. Figure 4(a) shows the pre-edge region of the Ti K-edge XANES spectra. Based on the dipole slection rule, these spectral features at the K edge are due to transitions from the Ti 1s core level to 4p-derived final states, which are composed of strongly hybridized O 2p and Ti 4sp and 3d orbitals. In the TM oxide system, generally, the quadrupole-allowed transitions occur in the pre-edge region, which corresponds to the contribution from 3d orbitals through 4sp–3d hybridization [24, 28–30]. For a detailed comparison of the pre-edge spectra, a Gaussian function was subtracted from the original Ti K-edge spectrum, as shown in the inset of figure 4(a). Thus, the Ti K-edge spectra of samples LTO and LTVO with x over the entire doping range (0.005–0.02) are displayed in figure 4(a). For the LTVO at dilute concentration with $x = 0.005$–0.01, the spectra are similar to that of LTO with the same photon energy at the main peak A_3, as marked by the black arrow in figure 4(a). The valence appears to remain as +3.5 because of the smaller concentration of V doping; however, as the doping level is increased to $x = 0.015$ and 0.02, the intensity pre-peak spectrum increases when compared to that of pure LTO. A chemical shift is also observed as concentration increases, as indicated by the red arrow in figure 4(a). Figure 4(b) shows the pre-edge region between 4969 and 4977 eV of Ti K-edge XANES spectra of TiO_2 (anatase) and LTVO ($x = 0$, 0.02) samples. The spectrum clearly shows three main features (C_3, D_3 and E_3) in the pre-peak region of the TiO_2 (Ti^{4+}) spectrum. It has been indicated that the origin of these splittings of pre-peaks results from local excitations (1s to 3d t_{2g} and e_g) [30–33]. However, recently it has been suggested that most of the contribution to this splitting arises from the edge and corner sharing Ti octahedral, which lead to non-local, intersite hybrid excitations. The Ti 4p states interact with next-nearest-neighbour 3d states (both t_{2g} and e_g) on the absorbing atom through O 2p states [34–36]. For compounds LTO and LTVO, the local structure of Ti also embraces the O_h symmetry, thus the pre-peak region (A_3 and B_3) can be described in terms of a similar scenario [34–36]. The intensity of these two pre-peaks changes with V concentration. In the V doped LTO, the substitution of Ti by V gives rise to a slight decrease in the lattice constants [7]. Thus a reduction of the Ti–O–Ti bond length results in increased overlap of the absorber and the first-nearest neighbours: Ti 4p–Ti 3d orbitals mediated by O ion. Thus, the intensity of these two pre-peaks is closely associated with the increased number of unoccupied first-nearest-neighbour Ti 3d states. Thus, as V concentration increases, the intersite hybrid peak intensity increases. As evident from the inset of figure 4(b), the variation in the area under the pre-peak implies the change of the 3d unoccupied states through the interaction of Ti 4p–O 2p–Ti 3d states. The above results strengthen the view that the Ti is in mixed-valence states between LTO and LTVO [6, 30]. Close inspection of spectra of LTO and LTVO ($x = 0.02$) reveals that the pre-peaks A_3 and B_3 are more intense in LTVO than in LTO and are accompanied by a chemical shift of the main peak to the higher energy side. The valence is hence increased when the V is doped. Furthermore, the average valences of Ti in the case of doped LTVO ($x = 0.015$ and 0.02) are estimated to be about +3.6, from a simple calculation and a fit of the ratio of areas under these spectral lines.

The O K-edge XANES provides useful information about the unoccupied density of states in TMO because of covalent

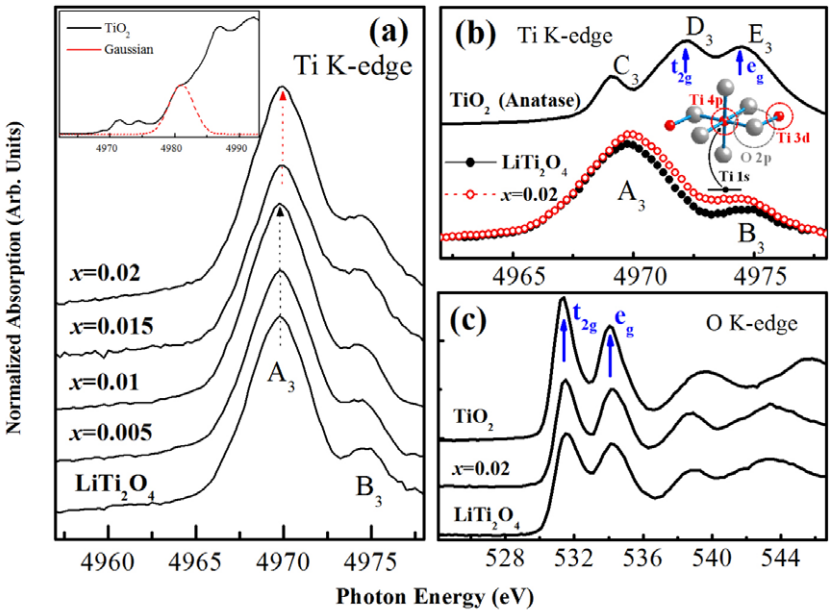

Figure 4. (a) Ti K-edge spectra of $LiTi_{2-x}V_xO_4$ ($x = 0$–0.2), TiO_2 and Ti_2O_3 in the pre-edge region. The inset shows the fitting used. (b) Detailed comparison of XANES at the Ti K edge mainly at the pre-edge region for $LiTi_{2-x}V_xO_4$ ($x = 0$ and 0.02) displayed. (c) O K-edge XANES spectra shown with two main peaks corresponding to O 2p–Ti 3d t_{2g} and e_g hybridized states.

mixing between O and TM ions. Figure 4(c) displays the O K-edge XANES spectra; the two features at around 530–536 eV are due to the strong Ti 3d–O 2p hybridizations and assigned to the 3d t_{2g} and e_g states, respectively. Similar to the increase in peak ratio t_{2g}/e_g as shown in Ti L-edge XANES, the intensities of peaks corresponding to t_{2g} and e_g states in the O K edge changes, suggesting strong Ti 3d–O 2p hybridization. In other words, all the above results coupled from XANES and RIXS spectroscopy strongly confirm that the Ti valence is enhanced as the doping level of V ions increases. Dilute doping of V results in a complete suppression of superconductivity of LTO resulting from the change in Ti–O hybridization and electron–electron correlation.

Spinel oxides of Ti and V belong to early 3d TMOs and have less hybridization between TM 3d and O 2p orbitals compared to late 3d TMOs because of the relatively large band gap between TM 3d and O 2p orbitals. As mentioned earlier, while spinel LVO shows a heavy fermionic behaviour with high electronic specific heat and a Curie–Weiss spin susceptibility, VTO is a spinel superconductor and the conduction takes place on the Ti sublattice via the t_{2g} orbitals with narrow bandwidth of the order of 2–3 eV, thus suggesting strong electronic correlations. The origin of their physics and the role of the spinel structure in their electronic properties are as yet unsolved issues. The present study provides the role of 3d electrons in their properties. The full solid solution of $LiTi_{2-x}V_xO_4$ ($0 \leqslant x \leqslant 2$) has been investigated [6]. Doping V at the Ti site changes the band gap and d-electron exchange in Ti levels to maintain electrical neutrality. Many mechanisms have been proposed to understand the rapid suppression of superconductivity with dilute doping of V in LTO. Dilute V doping in LTO may result in two major electronic effects. One is a simple pair-breaking effect due to dilute V doping with electron spin $\Delta S = 1$ on the superconductivity [6, 37]. The other is the carrier doping effect on electron correlation through band filling. The 3d electrons of V are assumed to hybridize the Ti conduction electrons and then to be itinerant. It is commonly considered that the simple magnetic pair-breaking effect of additional impurity electron spin on the superconductivity may be responsible, assuming localized moments of the 3d electrons of V [6]. The localized magnetic moment per V atom is estimated to be 1.7 μ_B in the V^{4+} state with $S = 1/2$ [6]. However, XANES measurements at V K edges shown in figure 5 exhibit that the V is more like the 3+ state [38], which has d^2 configuration and is expected to provide very small magnetic moment, possibly due to the antiparallel orientation of electron spins. The reduction of the V magnetic moment is also evidenced in the spinel ZnV_2O_4 [39]. The second possible reason may be the reduction of charge carriers in Ti t_{2g} bands. In such case, the V electrons are expected to localize Ti conduction electrons. If Ti ions in LTO possess 3+ and 4+ valency states, then one expects ~0.5 (t_{2g}) electrons in the conduction band. This will result in the observation of d–d excitation in the energy range of 0–5 eV, due to the presence of these electrons in the t_{2g} (occupied state) to excite to either the t_{2g} (unoccupied) or e_g (unoccupied) states. If the Ti valence increases from +3 to +4 due to V doping, the number of electrons occupying the t_{2g} orbital is expected to decrease. Then the number of electrons to excite the t_{2g} electron into the t_{2g} or e_g states is expected to reduce. The above RIXS spectra reveal a significant variation in the d–d excitation feature which decreases dramatically as the LTO is doped even with dilute doping of V. This indicates a decrease of Ti 3d occupied states with the increase of V concentrations. In other words, the Ti t_{2g} occupation number is changed after V doping. Such valence variation is marginal in XANES spectra

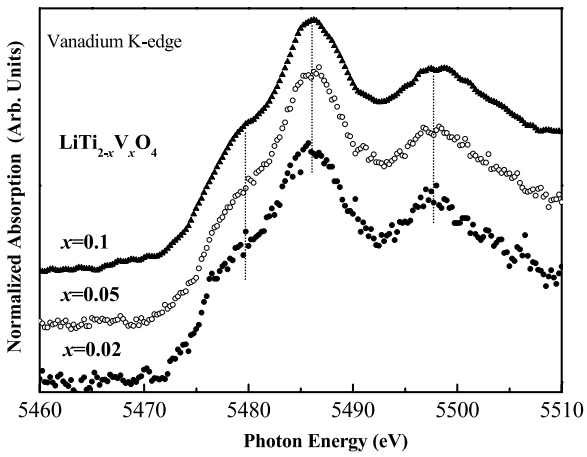

Figure 5. V K edge of $LiTi_{2-x}V_xO_4$ ($x = 0.02$) compared with higher doping ($x = 0.05$ and 0.1). The similarity of the spectral profile implies no significant change in the electronic structure around the V site.

at Ti K or L edges, but significant in RIXS spectra. The above experimental results, mainly the observation of reduction in the intensities of t_{2g}–t_{2g} and t_{2g}–e_g transitions from RIXS spectra, support the role of these electronic states in the rapid suppression of T_c in dilute V doped LTO. The present result thus supports that the reduction of density of states of Ti 3d electrons at Fermi level is responsible for rapid suppression of superconductivity.

4. Conclusion

The present study, using the XANES and RIXS spectroscopies, shows the mixed valency nature of Ti ions and significant variation in the hybridization of Ti 3d–O 2p states. The RIXS exhibits the low energy excitation due to d–d excitation, electron correlation and the increase in Ti valence consistent with the XANES results. The observed rapid suppression of superconductivity is attributed to change in density of states of Ti 3d electrons and Ti–O hybridization. The present study also demonstrated that RIXS is a powerful tool to investigate the electronic states and electron correlations of Ti compounds where the XANES spectral features are subdued.

Acknowledgments

The National Science Council of Taiwan (contracts NSC-98-2112-M-213-006-MY3 and NSC-099-2112-M-001-036-MY3) supported this work. We thank Dr J M Chen for beamline support and Dr J F Lee for useful discussions.

References

[1] Bussmann-Holder A and Keller H 2007 *High T_c Superconductors and Related Transition Metal Oxides* (Berlin *et al*: Springer)
[2] Merz M *et al* 1988 *Phys. Rev. Lett.* **80** 5192
[3] Johnston D C 1976 *J. Low Temp. Phys.* **25** 145
[4] Sun C P, Lin J Y, Mollah S, Ho P L, Yang H D, Hsu F C, Liao Y C and Wu M K 2004 *Phys. Rev.* B **70** 054519
[5] Wu M K *et al* under preparation
[6] Kichambare P, Kijima N, Honma H, Ebisu S and Nagata S 1996 *J. Phys. Chem. Solids* **57** 1615
[7] Hsu F C, Liao Y C, Yan D C, Gu S Y, Wu M K, Tang H Y and Perng T P 2007 *Physica* C **460** 546
[8] Xu F C, Liao Y C, Wang M J, Wu C T, Chiu K F and Wu M K 2003 *J. Low Temp. Phys.* **131** 569
[9] Cava R J, Murphy D W, Zahurak S, Santoro A and Roth R S 1984 *J. Solid State Chem.* **53** 64
[10] Ra W, Nakayama M, Uchimoto Y and Wakihara M 2005 *J. Phys. Chem.* B **109** 1130
[11] Millis A J 1998 *Nature* **392** 147
[12] Massidda S, Yu J and Freeman A J 1988 *Phys. Rev.* B **38** 11352
[13] Chen C L, Yeh K W, Huang D J, Hsu F C, Lee Y C, Huang S W, Guo G Y, Lin H J, Rao S M and Wu M K 2008 *Phys. Rev.* B **78** 214105
[14] De Groot F M F, Fuggle J C, Thole B T and Sawatzky G A 1990 *Phys. Rev.* B **41** 928
De Groot F M F, Fuggle J C, Thole B T and Sawatzky G A 1990 *Phys. Rev.* B **42** 5459
[15] Maddox B R, Lazicki A, Yoo C S, Iota V, Chen M, McMahan A K, Hu M Y, Chow P, Scalettar R T and Pickett W E 2006 *Phys. Rev. Lett.* **96** 215701
[16] Rueff J P, Hague C F, Mariot J M, Journel L, Delaunay R, Kappler J P, Schmerber G, Derory A, Jaouen N and Krill G 2004 *Phys. Rev. Lett.* **93** 067402
[17] Dallera C, Grioni M, Shukla A, Vankó G, Sarrao J L, Rueff J P and Cox D L 2002 *Phys. Rev. Lett.* **19** 196403
[18] Warwick T, Heimann P, Mossessian D, McKinney W and Padmore H 1995 *Rev. Sci. Instrum.* **66** 2037
[19] Nordgren J, Bray G, Cramm S, Nyholm R, Rubensson J E and Wassdahl N 1989 *Rev. Sci. Instrum.* **60** 1690
[20] Matsubara M, Uozumi T, Kotani A, Harada Y and Shin S 2002 *J. Phys. Soc. Japan* **71** 347
[21] Augustsson A, Henningsson A, Butorin S M, Siegbahn H, Nordgren J and Guo J-H 2003 *J. Chem. Phys.* **119** 3983
[22] Harada Y, Kinugasa T, Eguchi R, Matsubara M, Kotani A, Watanabe M, Yagishita A and Shin S 2000 *Phys. Rev.* B **61** 12854
[23] Agui A, Uozumi T, Mizumaki M and Käämbra T 2009 *Phys. Rev.* B **79** 092402
[24] Finkelstein L D, Zabolotzky E I, Korotin M A, Shamin S N, Butorin S M, Kurmaev E Z and Nordgren J 2002 *X-ray Spectrom.* **31** 414
[25] De Groot F M F, Faber J C, Michile J J M, Czyzyk M. T, Abbate M and Fuggle J C 1993 *Phys. Rev.* B **48** 2074
[26] Le Fevre P, Danger J, Magnan H, Chandesris D, Jupille J, Bourgeois S, Arrio M A, Gotter R, Verdini A and Morgante A 2004 *Phys. Rev.* B **69** 155421
[27] Richter J H, Henningsson A, Sanyal B, Karlsson P G, Andersson M P, Uvdal P, Siegbahn H, Eriksson O and Sandell A 2005 *Phys. Rev.* B **71** 235419
[28] Kucheyev S O 2004 *Phys. Rev.* B **69** 245102
[29] Poumellec B, Marucco J F and Touzelin B 1987 *Phys. Rev.* B **35** 2248
[30] Durmeyer O, Kappler J P, Beaurepaire E, Heintz J M and Drillon M 1990 *J. Phys.: Condens. Matter* **2** 6127
[31] Parlebas J C, Khan M A, Uozumi T, Okada K and Kotani A 1995 *J. Electron. Spectrosc. Relat. Phenom.* **71** 117
[32] Wu Z Y *et al* 1997 *Phys. Rev.* B **55** 10382
[33] Brydson R *et al* 1989 *J. Phys.: Condens. Matter* **1** 797
[34] Joly Y, Cabaret D, Renevier H and Natoli C R 1999 *Phys. Rev. Lett.* **82** 2398
[35] Uozumi T *et al* 1992 *Europhys. Lett.* **18** 85
[36] Cabaret D, Bordage A, Juhin A, Arfaoui M and Gaudry E 2010 *Phys. Chem. Chem. Phys.* **12** 5619
[37] Itoh Y, Moritsu N and Yoshimura K 2008 *J. Phys. Soc. Japan* **77** 123713
[38] Bordage A *et al* 2011 *Phys. Chem. Miner.* **38** 449
[39] Muhtar, Takagi F, Kawakami K and Tsuda N 1988 *J. Phys. Soc. Japan* **57** 3119